Published by Institute of Physics Publishing for SISSA

Received: *July 21, 2006*
Accepted: *August 9, 2006*
Published: *September 7, 2006*

Single inclusive distribution and two-particle correlations inside one jet at "modified leading logarithmic approximation" of quantum chromodynamics
II. Steepest descent evaluation at small x

Redamy Perez-Ramos

*Laboratoire de Physique Théorique et Hautes Energies**
Unité Mixte de Recherche UMR 7589
Université Pierre et Marie Curie-Paris 6;
CNRS;
Université Denis Diderot-Paris 7, France
E-mail: perez@lpthe.jussieu.fr

Abstract: The MLLA single inclusive distribution inside one high energy (gluon) jet at small x is estimated by the steepest descent method. Its analytical expression is obtained outside the "limiting spectrum". It is then used to evaluate 2-particle correlations at the same level of generality. The dependence of both observables on the ratio between the infrared cutoff Q_0 and $\Lambda_{\rm QCD}$ is studied. Fong & Webber's results for correlations are recovered at the limits when this ratio goes to 1 and when one stays close to the peak of the single inclusive distribution.

Keywords: QCD, Jets.

*LPTHE, tour 24-25, 5ème étage, Université P. et M. Curie, BP 126, 4 place Jussieu, F-75252 Paris Cedex 05 (France).

JHEP09(2006)014

Contents

1. Introduction

Exactly solving the MLLA evolution equations for the quark and gluon inclusive spectra and for 2-particle correlations inside one jet provided, at small x, in [1], analytical expressions for these observables, which were unfortunately limited, for technical reasons to the "limiting spectrum" $\lambda \equiv \ln(Q_0/\Lambda_{\rm QCD}) = 0$. The goal of this second work is to go

JHEP09(2006)014

beyond this limit in an approximate scheme which proves very economical and powerful: the steepest descent (SD) method. It offers sizable technical progress in the calculation of both observables.

First, we perform a SD evaluation of the (quark and) gluon single inclusive distributions. Their full dependence on λ is given, including the normalization. The well known shift to smaller values of x of the maximum of the distribution, as compared with DLA calculations is checked, as well as its Gaussian shape around the maximum. Comparison with the results obtained numerically in [2] is done.

As shown in [1], knowing the logarithmic derivatives of the inclusive spectra immediately gives access to 2-particle correlations. This is accordingly our next step. Since, in particular, the former prove to be infra-red stable in the limit $\lambda \to 0$, the result can be safely compared with the exact one obtained in [1]. The agreement turns out to be excellent, and increases with the energy scale of the process.

Last, we evaluate 2-particle correlations inside one high energy jet and study their behavior at $Q_0 \neq \Lambda_{\rm QCD}$. That one recovers the results of Fong & Webber [3] close to the peak of the single inclusive distribution and when $\lambda \to 0$ is an important test of the validity and efficiency of the SD method. The quantitative predictions do not substantially differ from the ones of [1] for the "limiting spectrum", which stays the best candidate to reproduce experimental results.

A conclusion summarizes the achievements, limitations and expectations of [1] and of the present work. It is completed with two technical appendices.

2. Steepest descent evaluation of the single inclusive distribution

We consider the production of one hadron inside a quark or a gluon jet in a hard process. It carries the fraction x of the total energy E of the jet. Θ_0 is the half opening angle of the jet while Θ is the angle corresponding to the first splitting with energy fraction $x \ll z \ll 1$.

2.1 Variables and kinematics

The variables and kinematics of the process under consideration are the same as in section 3.1 of [1].

2.2 Evolution equations for particle spectra at MLLA

We define like in [1] the logarithmic parton densities

$$Q(\ell) \equiv xD_Q(x), \qquad G(\ell) = xD_G(x)$$

for quark and gluon jets in terms of which the system of evolution equations for particle spectra at small x (see eqs. (42) and (43) of [1]) read

$$Q(\ell, y) = \delta(\ell) + \frac{C_F}{N_c}\int_0^\ell d\ell' \int_0^y dy' \gamma_0^2(\ell' + y')\Big(1 - \frac{3}{4}\delta(\ell' - \ell)\Big)G(\ell', y'), \tag{2.1}$$

$$G(\ell, y) = \delta(\ell) + \int_0^\ell d\ell' \int_0^y dy' \gamma_0^2(\ell' + y')\Big(1 - a\delta(\ell' - \ell)\Big)G(\ell', y'), \tag{2.2}$$

where

$$a=\frac{1}{4N_c}\left[\frac{11}{3}N_c+\frac{4}{3}n_fT_R\left(1-\frac{2C_F}{N_c}\right)\right]\overset{n_f=3}{=}0.935. \tag{2.3}$$

The terms $\propto \frac{3}{4}$ in (2.1) and $\propto a$ in (2.2) account for hard corrections to soft gluon multiplication, sub-leading $g\to q\bar{q}$ splittings, strict angular ordering and energy conservation.

2.3 Evolution equations; steepest descent evaluation

The exact solution of (2.2) is demonstrated in [1] to be given by the Mellin's integral representation

$$\begin{aligned}G(\ell,y)&=(\ell+y+\lambda)\iint\frac{d\omega\,d\nu}{(2\pi i)^2}e^{\omega\ell+\nu y}\int_0^\infty\frac{ds}{\nu+s}\left(\frac{\omega\,(\nu+s)}{(\omega+s)\,\nu}\right)^{1/\beta(\omega-\nu)}\left(\frac{\nu}{\nu+s}\right)^{a/\beta}e^{-\lambda s}\\&=(\ell+y+\lambda)\iint\frac{d\omega\,d\nu}{(2\pi i)^2}e^{\omega\ell+\nu y}\int_0^\infty\frac{ds}{\nu+s}\left(\frac{\nu}{\nu+s}\right)^{a/\beta}e^{\sigma(s)},\end{aligned} \tag{2.4}$$

where we have exponentiated the kernel (symmetrical in (ω,ν))

$$\sigma(s)=\frac{1}{\beta(\omega-\nu)}\ln\left(\frac{\omega(\nu+s)}{\nu(\omega+s)}\right)-\lambda s. \tag{2.5}$$

Eq. (2.4) will be estimated by the SD method. The value s_0 of the saddle point, satisfying $\left.\frac{d\sigma(s)}{ds}\right|_{s=s_0}=0$, reads (see [7])

$$s_0(\omega,\nu)=\frac{1}{2}\left[\sqrt{\frac{4}{\beta\lambda}+(\omega-\nu)^2}-(\omega+\nu)\right]. \tag{2.6}$$

One makes a Taylor expansion of $\sigma(s)$ nearby s_0:

$$\sigma(s)=\sigma(s_0)+\frac{1}{2}\sigma''(s_0)(s-s_0)^2+\mathcal{O}\left((s-s_0)^2\right),\quad \sigma''(s_0)=-\beta\lambda^2\sqrt{\frac{4}{\beta\lambda}+(\omega-\nu)^2}<0, \tag{2.7}$$

such that

$$\int_0^\infty\frac{ds}{\nu+s}\left(\frac{\omega\,(\nu+s)}{(\omega+s)\,\nu}\right)^{1/\beta(\omega-\nu)}\left(\frac{\nu}{\nu+s}\right)^{a/\beta}e^{-\lambda s}\overset{\lambda\gg1}{\approx}2\sqrt{\frac{\pi}{2}}\frac{e^{\sigma(s_0)}}{(\nu+s_0)\sqrt{|\,\sigma''(s_0)\,|}}\left(\frac{\nu}{\nu+s_0}\right)^{a/\beta}. \tag{2.8}$$

The condition $\lambda\gg1\Rightarrow\alpha_s/\pi\ll1$ [1] guarantees, in particular, the convergence of the perturbative approach. Substituting (2.8) in (2.4) yields

$$G(\ell,y)\approx2\sqrt{\frac{\pi}{2}}(\ell+y+\lambda)\iint\frac{d\omega\,d\nu}{(2\pi i)^2}\,\frac{e^{\phi(\omega,\nu,\ell,y)}}{(\nu+s_0)\sqrt{|\,\sigma''(s_0)\,|}}\left(\frac{\nu}{\nu+s_0}\right)^{a/\beta}, \tag{2.9}$$

where the argument of the exponential is

$$\phi(\omega,\nu,\ell,y)=\omega\ell+\nu y+\frac{1}{\beta\,(\omega-\nu)}\ln\frac{\omega\,(\nu+s_0)}{(\omega+s_0)\,\nu}-\lambda s_0. \tag{2.10}$$

[1] in (2.7), λ appears to the power $3/2>1$, which guarantees the fast convergence of the SD as λ increases.

Once again, we perform the SD method to evaluate (2.9). The saddle point (ω_0, ν_0) satisfies the equations

$$\frac{\partial\phi}{\partial\omega} = \ell - \frac{1}{\beta\left(\omega-\nu\right)^2}\ln\frac{\omega\left(\nu+s_0\right)}{\left(\omega+s_0\right)\nu} + \frac{1}{\beta\omega\left(\omega-\nu\right)} - \lambda\frac{\left(\nu+s_0\right)}{\left(\omega-\nu\right)} = 0, \tag{2.11a}$$

$$\frac{\partial\phi}{\partial\nu} = y + \frac{1}{\beta\left(\omega-\nu\right)^2}\ln\frac{\omega\left(\nu+s_0\right)}{\left(\omega+s_0\right)\nu} - \frac{1}{\beta\nu\left(\omega-\nu\right)} + \lambda\frac{\left(\omega+s_0\right)}{\left(\omega-\nu\right)} = 0. \tag{2.11b}$$

Adding and subtracting (2.11a) and (2.11b) gives respectively

$$\omega_0\nu_0 = \frac{1}{\beta\left(\ell+y+\lambda\right)}, \tag{2.12a}$$

$$y-\ell = \frac{1}{\beta\left(\omega_0-\nu_0\right)}\left(\frac{1}{\omega_0}+\frac{1}{\nu_0}\right) - \frac{2}{\beta\left(\omega_0-\nu_0\right)^2}\ln\frac{\omega_0\left(\nu_0+s_0\right)}{\left(\omega_0+s_0\right)\nu_0} - \lambda\frac{\omega_0+\nu_0+2s_0}{\omega_0-\nu_0}; \tag{2.12b}$$

(ω_0, ν_0) also satisfies (from (2.6))

$$\left(\omega_0+s_0\right)\left(\nu_0+s_0\right) = \frac{1}{\beta\lambda}. \tag{2.13}$$

One can substitute the expressions (2.11a) and (2.11b) of ℓ and y into (2.10), which yields

$$\varphi \equiv \phi(\omega_0,\nu_0,\ell,y) = \frac{2}{\beta\left(\omega_0-\nu_0\right)}\ln\frac{\omega_0\left(\nu_0+s_0\right)}{\left(\omega_0+s_0\right)\nu_0}. \tag{2.14}$$

Introducing the variables (μ, υ) [7] to parametrize (ω_0, ν_0) through

$$\omega_0\left(\nu_0\right) = \frac{1}{\sqrt{\beta(\ell+y+\lambda)}}e^{\pm\mu(\ell,y)}, \qquad \left(\omega_0+s_0\right)\left(\nu_0+s_0\right) = \frac{1}{\sqrt{\beta\lambda}}e^{\pm\upsilon(\ell,y)}, \tag{2.15}$$

one rewrites (2.14) and (2.12b) respectively in the form

$$\varphi(\mu,\upsilon) = \frac{2}{\sqrt{\beta}}\left(\sqrt{\ell+y+\lambda}-\sqrt{\lambda}\right)\frac{\mu-\upsilon}{\sinh\mu-\sinh\upsilon}, \tag{2.16}$$

$$\frac{y-\ell}{y+\ell} = \frac{\left(\sinh 2\mu-2\mu\right)-\left(\sinh 2\upsilon-2\upsilon\right)}{2\left(\sinh^2\mu-\sinh^2\upsilon\right)}; \tag{2.17a}$$

moreover, since $\omega_0-\nu_0 = \left(\omega_0-s_0\right)-\left(\nu_0-s_0\right)$, (μ, υ) also satisfy

$$\frac{\sinh\upsilon}{\sqrt{\lambda}} = \frac{\sinh\mu}{\sqrt{\ell+y+\lambda}}. \tag{2.17b}$$

Performing a Taylor expansion of $\phi(\omega,\nu,\ell,y)$ around (ω_0,ν_0), which needs evaluating $\frac{\partial^2\phi}{\partial\omega^2}$, $\frac{\partial^2\phi}{\partial\nu^2}$ and $\frac{\partial^2\phi}{\partial\omega\partial\nu}$ (see appendix A.1), treating $(Y+\lambda)$ as a large parameter and making use of (2.15) provides the SD result

$$G(\ell,y) \approx \mathcal{N}(\mu,\upsilon,\lambda)\exp\left[\frac{2}{\sqrt{\beta}}\left(\sqrt{\ell+y+\lambda}-\sqrt{\lambda}\right)\frac{\mu-\upsilon}{\sinh\mu-\sinh\upsilon}+\upsilon-\frac{a}{\beta}(\mu-\upsilon)\right], \tag{2.18}$$

where

$$\mathcal{N}(\mu,\upsilon,\lambda)=\frac{1}{2}(\ell{+}y{+}\lambda)\frac{\left(\frac{\beta}{\lambda}\right)^{1/4}}{\sqrt{\pi\cosh\upsilon\ \mathrm{Det}\,A(\mu,\upsilon)}}\left(\frac{\lambda}{\ell+y+\lambda}\right)^{a/2\beta}$$

with (see details in appendix A.1)

$$\mathrm{Det}\,A(\mu,\nu)=\beta\,(\ell{+}y{+}\lambda)^3\left[\frac{(\mu{-}\upsilon)\cosh\mu\cosh\upsilon{+}\cosh\mu\sinh\upsilon{-}\sinh\mu\cosh\upsilon}{\sinh^3\mu\cosh\upsilon}\right]. \quad (2.19)$$

2.3.1 Shape of the spectrum given in eq. (2.18)

We normalize (2.18) by the MLLA mean multiplicity inside one jet [8]

$$\bar{n}(Y)\overset{\lambda\gg1}{\approx}\frac{1}{2}\left(\frac{Y+\lambda}{\lambda}\right)^{-\frac{1}{2}\frac{a}{\beta}+\frac{1}{4}}\exp\left[\frac{2}{\sqrt{\beta}}\left(\sqrt{Y+\lambda}-\sqrt{\lambda}\right)\right].$$

The normalized expression for the single inclusive distribution as a function of $\ell=\ln(1/x)$ is accordingly obtained by setting $y=Y-\ell$ in (2.18)

$$\frac{G(\ell,Y)}{\bar{n}(Y)}\approx\sqrt{\frac{\beta^{1/2}(Y+\lambda)^{3/2}}{\pi\cosh\upsilon\,\mathrm{Det}\,A(\mu,\upsilon)}}\exp\left[\frac{2}{\sqrt{\beta}}\left(\sqrt{Y+\lambda}-\sqrt{\lambda}\right)\right.$$
$$\left.\times\left(\frac{\mu-\upsilon}{\sinh\mu-\sinh\upsilon}-1\right)+\upsilon-\frac{a}{\beta}(\mu-\upsilon)\right]. \quad (2.20)$$

One can explicitly verify that (2.20) preserves the position of the maximum [8 – 10] at

$$\ell_{\max}=\frac{Y}{2}+\frac{1}{2}\frac{a}{\beta}\left(\sqrt{Y+\lambda}-\sqrt{\lambda}\right)>\frac{Y}{2}, \quad (2.21)$$

as well as the gaussian shape of the distribution around (2.21) (see appendix A.2)

$$\frac{G(\ell,Y)}{\bar{n}(Y)}\approx\left(\frac{3}{\pi\sqrt{\beta}\left[(Y+\lambda)^{3/2}-\lambda^{3/2}\right]}\right)^{1/2}\exp\left(-\frac{2}{\sqrt{\beta}}\frac{3}{(Y+\lambda)^{3/2}-\lambda^{3/2}}\frac{(\ell-\ell_{\max})^2}{2}\right). \quad (2.22)$$

In figure 1 we compare for $Y=10$ and $\lambda=2.5$ the MLLA curve with DLA (by setting $a=0$ in (2.20)). The general features of the MLLA curve (2.20) at $\lambda\neq0$ are in good agreement with those of [2].

The shape of the single inclusive spectrum given by (2.20) can easily be proved to be "infrared stable" (it has indeed a final limit when $\lambda\to0$).

2.4 Logarithmic derivatives

Their calculation is important since they appear in the expressions of 2-particle correlations.

Exponentiating the (ℓ,y) dependence of the factor $\mathcal{N}$ in (2.18), we decompose the whole expression in two pieces

$$\psi=\varphi+\delta\psi, \quad (2.23)$$

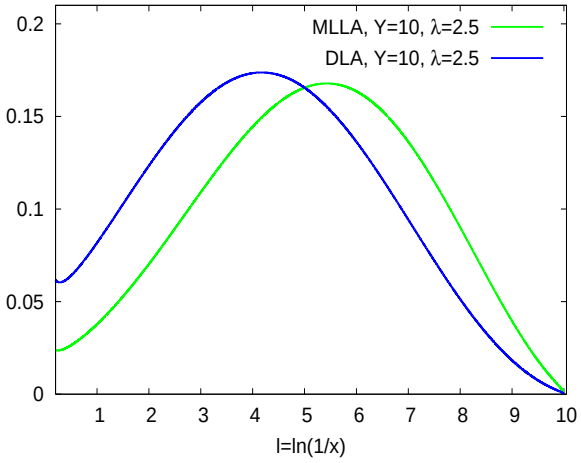

Figure 1: SD normalized spectrum: DLA (blue), MLLA (green); $Y = 10.0$, $\lambda = 2.5$.

where φ, given in (2.16), is the DLA term for the shape of the distribution [7], and

$$\delta\psi = -\frac{1}{2}\left(1+\frac{a}{\beta}\right)\ln(\ell+y+\lambda) - \frac{a}{\beta}\mu + \left(1+\frac{a}{\beta}\right)\upsilon + \frac{1}{2}\ln[Q(\mu,\upsilon)] \tag{2.24}$$

is the sub-leading contribution (in the sense that its derivative gives the MLLA correction), where

$$Q(\mu,\upsilon) \equiv \frac{\beta(\ell+y+\lambda)^3}{\cosh\upsilon\,\mathrm{Det}\;A(\mu,\upsilon)} = \frac{\sinh^3\mu}{(\mu-\upsilon)\cosh\mu\cosh\upsilon+\cosh\mu\sinh\upsilon-\sinh\mu\cosh\upsilon}.$$

By the definition of the saddle point, the derivatives of (2.16) over ℓ and y respectively read:

$$\varphi_\ell = \omega_0 = \gamma_0 e^{\mu}, \qquad \varphi_y = \nu_0 = \gamma_0 e^{-\mu}. \tag{2.25}$$

We introduce (see appendix A.3)

$$\begin{aligned} \mathcal{L}(\mu,\upsilon) &= -\frac{a}{\beta} + L(\mu,\upsilon), & L(\mu,\upsilon) &= \frac{1}{2}\frac{\partial}{\partial\mu}\ln[Q(\mu,\upsilon)], \\ \mathcal{K}(\mu,\upsilon) &= 1 + \frac{a}{\beta} + K(\mu,\upsilon), & K(\mu,\upsilon) &= \frac{1}{2}\frac{\partial}{\partial\upsilon}\ln[Q(\mu,\upsilon)] \end{aligned} \tag{2.26}$$

and make use of

$$\frac{\partial\upsilon}{\partial\ell} = \tanh\upsilon\left(\coth\mu\frac{\partial\mu}{\partial\ell} - \frac{1}{2}\beta\gamma_0^2\right), \qquad \frac{\partial\upsilon}{\partial y} = \tanh\upsilon\left(\coth\mu\frac{\partial\mu}{\partial y} - \frac{1}{2}\beta\gamma_0^2\right),$$

that follows from (2.17b), to write $\delta\psi_\ell$, $\delta\psi_y$ in terms of $\frac{\partial\mu}{\partial\ell}$, $\frac{\partial\mu}{\partial y}$

$$\delta\psi_\ell = -\frac{1}{2}\left(1+\frac{a}{\beta}+\tanh\upsilon\,\mathcal{K}(\mu,\upsilon)\right)\beta\gamma_0^2 + \left(\mathcal{L}(\mu,\upsilon)+\tanh\upsilon\coth\mu\,\mathcal{K}(\mu,\upsilon)\right)\frac{\partial\mu}{\partial\ell}, \tag{2.27a}$$

$$\delta\psi_y = -\frac{1}{2}\left(1+\frac{a}{\beta}+\tanh\upsilon\,\mathcal{K}(\mu,\upsilon)\right)\beta\gamma_0^2 + \left(\mathcal{L}(\mu,\upsilon)+\tanh\upsilon\coth\mu\,\mathcal{K}(\mu,\upsilon)\right)\frac{\partial\mu}{\partial y}. \tag{2.27b}$$

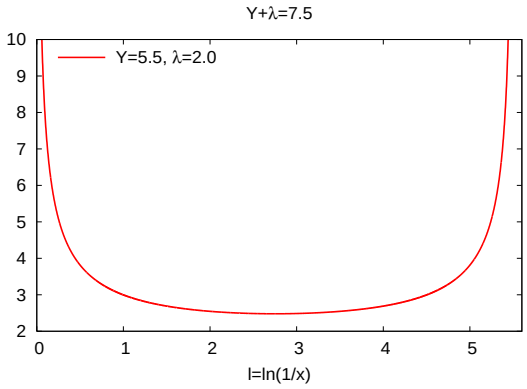

Figure 2: Behavior of $\widetilde{Q}(\mu,\upsilon)$ as a function of $\ell=\ln(1/x)$.

Using (2.17a) and (2.17b) we obtain

$$\frac{\partial\mu}{\partial\ell}=-\frac{1}{2}\beta\gamma_0^2\left[1+e^{\mu}\widetilde{Q}(\mu,\upsilon)\right],\qquad \frac{\partial\mu}{\partial y}=\frac{1}{2}\beta\gamma_0^2\left[1+e^{-\mu}\widetilde{Q}(\mu,\upsilon)\right] \tag{2.28}$$

where

$$\widetilde{Q}(\mu,\upsilon)=\frac{\cosh\mu\sinh\mu\cosh\upsilon-(\mu-\upsilon)\cosh\upsilon-\sinh\upsilon}{(\mu-\upsilon)\cosh\mu\cosh\upsilon+\cosh\mu\sinh\upsilon-\sinh\mu\cosh\upsilon}, \tag{2.29}$$

which we have displayed in figure 2 (useful for correlations).

Inserting (2.27b) and (2.28) into (2.27a) gives the SD logarithmic derivatives of the single inclusive distribution

$$\begin{aligned}\psi_\ell(\mu,\upsilon)\,=\,&\gamma_0e^{\mu}+\frac{1}{2}a\gamma_0^2\Big[e^{\mu}\widetilde{Q}(\mu,\upsilon)-\tanh\upsilon-\tanh\upsilon\coth\mu\Big(1+e^{\mu}\widetilde{Q}(\mu,\upsilon)\Big)\Big]\\&-\frac{1}{2}\beta\gamma_0^2\Big[1+\tanh\upsilon\Big(1+K(\mu,\upsilon)\Big)+C(\mu,\upsilon)\Big(1+e^{\mu}\widetilde{Q}(\mu,\upsilon)\Big)\Big]+\mathcal{O}(\gamma_0^2)\end{aligned} \tag{2.30a}$$

$$\begin{aligned}\psi_y(\mu,\upsilon)\,=\,&\gamma_0e^{-\mu}-\frac{1}{2}a\gamma_0^2\Big[2+e^{-\mu}\widetilde{Q}(\mu,\upsilon)+\tanh\upsilon-\tanh\upsilon\coth\mu\Big(1+e^{-\mu}\widetilde{Q}(\mu,\upsilon)\Big)\Big]\\&-\frac{1}{2}\beta\gamma_0^2\Big[1+\tanh\upsilon\Big(1+K(\mu,\upsilon)\Big)-C(\mu,\upsilon)\Big(1+e^{-\mu}\widetilde{Q}(\mu,\upsilon)\Big)\Big]+\mathcal{O}(\gamma_0^2)\end{aligned} \tag{2.30b}$$

where we have introduced (L and K have been written in (A.7) and (A.8))

$$C(\mu,\upsilon)=L(\mu,\upsilon)+\tanh\upsilon\coth\mu\Big(1+K(\mu,\upsilon)\Big). \tag{2.31}$$

C does not diverge when $\mu\sim\upsilon\to0$. One has indeed

$$\lim_{\mu,\upsilon\to0}\left[L(\mu,\upsilon)+\tanh\upsilon\coth\mu K(\mu,\upsilon)\right]=\lim_{\mu,\upsilon\to0}\frac{2-3\frac{\upsilon^2}{\mu^2}-\frac{\upsilon^3}{\mu^3}}{4\left(1-\frac{\upsilon^3}{\mu^3}\right)}\mu=0$$

as well as

$$\lim_{\mu,\upsilon\to0}\tanh\upsilon\coth\mu\left(1+e^{\pm\mu}\widetilde{Q}(\mu,\upsilon)\right)=\lim_{\mu,\upsilon\to0}=\frac{3\frac{\upsilon}{\mu}}{1-\frac{\upsilon^3}{\mu^3}}=\frac{3\sqrt{\frac{\lambda}{Y+\lambda}}}{1-\left(\frac{\lambda}{Y+\lambda}\right)^{3/2}}.$$

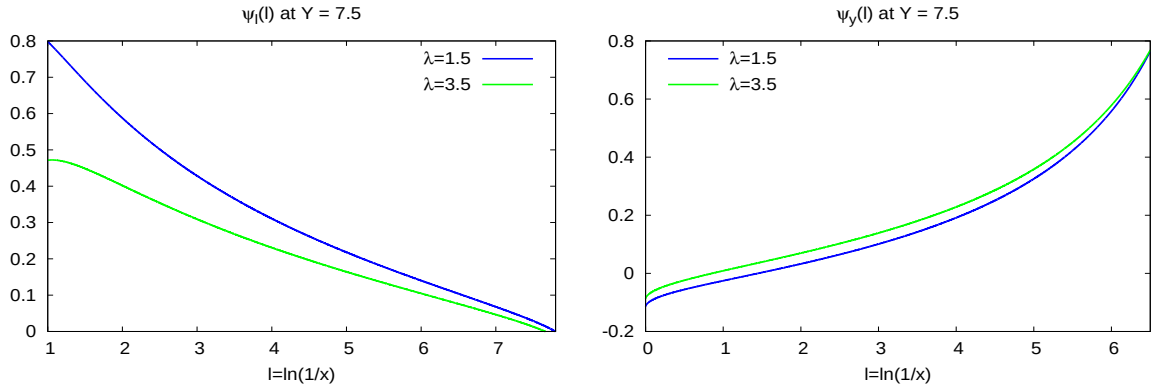

Figure 3: SD logarithmic derivatives ψ_ℓ and ψ_y of the inclusive spectrum at $Y = 7.5$, for $\lambda = 1.5$ and $\lambda = 3.5$.

In (2.30a) and (2.30b) it is easy to keep trace of leading and sub-leading contributions. The first $\mathcal{O}(\gamma_0)$ term is DLA [7] while the second ($\propto a \to$ "hard corrections") and third ($\propto \beta \to$ "running coupling effects") terms are MLLA corrections ($\mathcal{O}(\gamma_0^2)$), of relative order $\mathcal{O}(\gamma_0)$ with respect to the leading one. In figure 3 we plot (2.30a) (left) and (2.30b) (right) for two different values of λ; one observes that ψ_ℓ (ψ_y) decreases (increases) when λ increases.

For further use in correlations, the logarithmic derivatives have the important property that they do not depend on the normalization but only on the shape of the single inclusive distribution.

2.4.1 "Limiting spectrum": $\lambda \to 0$ ($Q_0 = \Lambda_{\rm QCD}$)

Since the logarithmic derivatives are "infrared stable" (see above), we can take the limit $\lambda \to 0$ in (2.30a) (2.30b),[2] and compare their shapes with the ones obtained in [5]; this is done in figures 4 and 5, at LEP-I energy ($E\Theta_0 = 91.2\,\text{GeV}$, $Y = 5.2$) and at the unrealistic value $Y = 15$.

The agreement between the SD and the exact logarithmic derivatives is seen to be quite good. The small deviations ($\leq 20\%$) that can be observed at large ℓ (the domain we deal with) arise from NMLLA corrections that one does not control in the exact solution. The agreement gets better and better as the energy increases.

It is checked in appendix (A.4) that (2.18) satisfies the evolution equation (2.2); the SD logarithmic derivatives (2.30a) and (2.30b) can therefore be used in the approximate calculation of 2-particle correlations at $\lambda \neq 0$. This is what is done in the next section.

3. 2-Particle correlations inside one jet at $\lambda \neq 0$ ($Q_0 \neq \Lambda_{\rm QCD}$)

We study the correlation between 2-particles inside one jet of half opening angle Θ within the MLLA accuracy. They have fixed energies $x_1 = \omega_1/E$, $x_2 = \omega_2/E$ ($\omega_1 > \omega_2$) and

[2]For this purpose, (2.17a) has been numerically inverted.

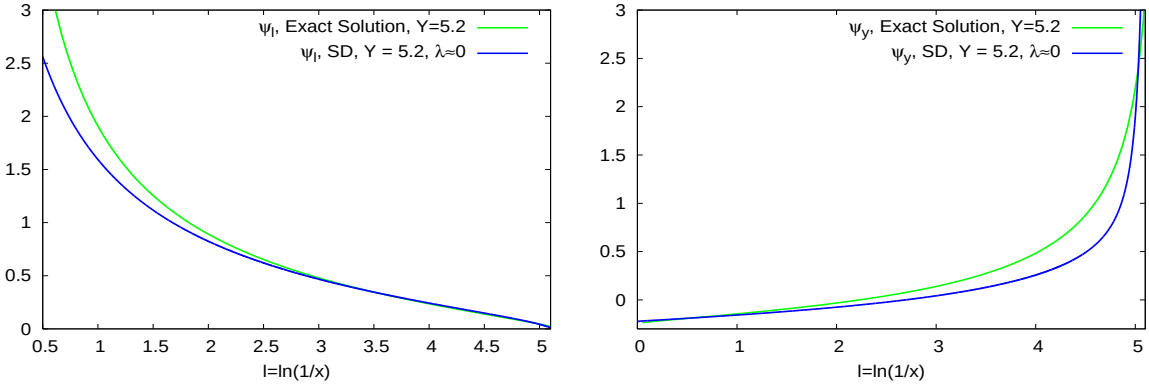

Figure 4: SD logarithmic derivatives ψ_ℓ (left) and ψ_y (right) compared with the ones of [1] at $Y = 5.2$.

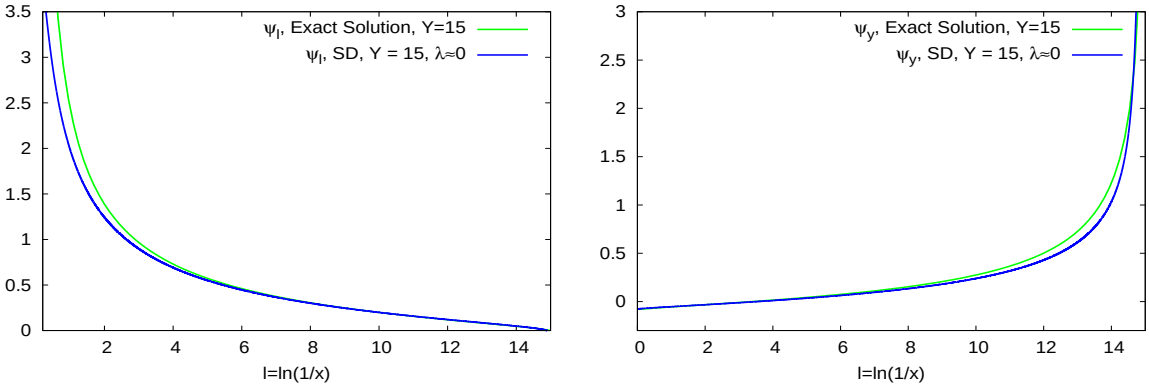

Figure 5: SD logarithmic derivatives ψ_ℓ (left) and ψ_y (right) compared with the ones of [1] at $Y = 15$.

are emitted at arbitrary angles Θ_1, Θ_2. The constrain $\Theta_1 \geq \Theta_2$ follows from the angular ordering in the cascading process. One has $\Theta \geq \Theta_1$ (see figure 1 of [1]).

3.1 Variables and kinematics

The variables and kinematics of the cascading process are defined like in section 3.2 of [1].

3.2 MLLA evolution equations for correlations

The system of integral evolution equations for the quark and gluon jets two-particle correlation reads (see eqs. (65) and (66) of [1])

$$Q^{(2)}(\ell_1, y_2, \eta) - Q_1(\ell_1, y_1)Q_2(\ell_2, y_2) = \frac{C_F}{N_c}\int_0^{\ell_1} d\ell \int_0^{y_2} dy\, \gamma_0^2(\ell + y) \times \left[1 - \frac{3}{4}\delta(\ell - \ell_1)\right] G^{(2)}(\ell, y, \eta), \tag{3.1}$$

$$G^{(2)}(\ell_1,y_2,\eta)-G_1(\ell_1,y_1)G_2(\ell_2,y_2)=\int_0^{\ell_1}d\ell\int_0^{y_2}dy\,\gamma_0^2(\ell+y)\Big[1-a\delta(\ell-\ell_1)\Big]G^{(2)}(\ell,y,\eta)$$
$$+(a-b)\int_0^{y_2}dy\,\gamma_0^2(\ell_1+y)G(\ell_1,y+\eta)G(\ell_1+\eta,y). \tag{3.2}$$

a is defined in (2.3) while

$$b=\frac{1}{4N_c}\left[\frac{11}{3}N_c-\frac{4}{3}n_fT_R\left(1-2\frac{C_F}{N_c}\right)^2\right]\overset{n_f=3}{=}0.915. \tag{3.3}$$

3.3 MLLA solution at $\lambda\neq 0$

The quark and gluon jet correlators $\mathcal{C}_q$ and $\mathcal{C}_g$ have been exactly determined for any λ in [1] by respectively setting $Q^{(2)}=\mathcal{C}_qQ_1Q_2$ and $G^{(2)}=\mathcal{C}_gG_1G_2$ into (3.1) and (3.2). In the present work we limit ourselves to the exact MLLA solution which consists in neglecting all $\mathcal{O}(\gamma_0^2)$ corrections in equations (64) and (84) of [1].

3.3.1 Gluon jet

At MLLA, the logarithmic derivatives of ψ (2.23) can be truncated to the saddle point derivatives φ_ℓ, φ_y of (2.16). The MLLA solution of (3.2) then reads (see (77) in [1])

$$\mathcal{C}_g-1\overset{MLLA}{\approx}\frac{1-b\,(\varphi_{1,\ell}+\varphi_{2,\ell})-\delta_1}{1+\bar\Delta+\Delta'+\delta_1} \tag{3.4}$$

where we introduce

$$\bar\Delta=\gamma_0^{-2}\Big(\varphi_{1,\ell}\varphi_{2,y}+\varphi_{1,y}\varphi_{2,\ell}\Big), \tag{3.5}$$
$$\Delta'=\gamma_0^{-2}\Big(\varphi_{1,\ell}\delta\psi_{2,y}+\delta\psi_{1,y}\varphi_{2,\ell}+\delta\psi_{1,\ell}\varphi_{2,y}+\varphi_{1,y}\delta\psi_{2,\ell}\Big); \tag{3.6}$$
$$\chi=\ln\left(1+\frac{1}{1+\bar\Delta}\right),\quad \chi_\ell=\frac{1}{\chi}\frac{\partial\chi}{\partial\ell},\quad \chi_y=\frac{1}{\chi}\frac{\partial\chi}{\partial y}; \tag{3.7}$$
$$\delta_1=\gamma_0^{-2}\Big[\chi_\ell(\varphi_{1,y}+\varphi_{2,y})+\chi_y(\varphi_{1,\ell}+\varphi_{2,\ell})\Big]. \tag{3.8}$$

(3.5) is obtained by using (2.25):

$$\bar\Delta(\mu_1,\mu_2)=2\cosh(\mu_1-\mu_2)=\mathcal{O}(1), \tag{3.9}$$

which is the DLA contribution [7], while (3.6) (see appendix B) is obtained by using (2.25), (2.27a) and (2.27b)

$$\Delta'(\mu_1,\mu_2)=\frac{e^{-\mu_1}\delta\psi_{2,\ell}+e^{-\mu_2}\delta\psi_{1,\ell}+e^{\mu_1}\delta\psi_{2,y}+e^{\mu_2}\delta\psi_{1,y}}{\gamma_0}=\mathcal{O}(\gamma_0); \tag{3.10}$$

it is a next-to-leading (MLLA) correction. To get (3.7), we first use (3.9), which gives

$$\chi_\ell=-\frac{\tanh\frac{\mu_1-\mu_2}{2}}{1+2\cosh(\mu_1-\mu_2)}\left(\frac{\partial\mu_1}{\partial\ell}-\frac{\partial\mu_2}{\partial\ell}\right),$$

$$\chi_y = -\frac{\tanh\frac{\mu_1-\mu_2}{2}}{1+2\cosh(\mu_1-\mu_2)}\left(\frac{\partial\mu_1}{\partial y}-\frac{\partial\mu_2}{\partial y}\right), \tag{3.11}$$

and then (2.28) to get

$$\chi_\ell = \beta\gamma_0^2\,\frac{\tanh\frac{\mu_1-\mu_2}{2}}{1+2\cosh(\mu_1-\mu_2)}\,\frac{e^{\mu_1}\widetilde{Q}_1 - e^{\mu_2}\widetilde{Q}_2}{2},$$
$$\chi_y = -\beta\gamma_0^2\frac{\tanh\frac{\mu_1-\mu_2}{2}}{1+2\cosh(\mu_1-\mu_2)}\,\frac{e^{-\mu_1}\widetilde{Q}_1 - e^{-\mu_2}\widetilde{Q}_2}{2}$$

which are $\mathcal{O}(\gamma_0^2)$. They should be plugged into (3.8) together with (2.25), which gives

$$\delta_1 = \beta\gamma_0\frac{2\sinh^2\left(\frac{\mu_1-\mu_2}{2}\right)}{3+4\sinh^2\left(\frac{\mu_1-\mu_2}{2}\right)}\Big(\widetilde{Q}(\mu_1,\upsilon_1)+\widetilde{Q}(\mu_2,\upsilon_2)\Big) = \mathcal{O}(\gamma_0); \tag{3.12}$$

it is also a MLLA term. For $Q \gg Q_0 \geq \Lambda_{\rm QCD}$ we finally get,

$$\mathcal{C}_g(\ell_1,\ell_2,Y,\lambda) \overset{MLLA}{\approx} 1+\frac{1-b\gamma_0\left(e^{\mu_1}+e^{\mu_2}\right)-\delta_1}{1+2\cosh(\mu_1-\mu_2)+\Delta'(\mu_1,\mu_2)+\delta_1} \tag{3.13}$$

where the expression for Δ' (B.1) is written in appendix B. It is important to notice that $\delta_1 \simeq 0$ near $\ell_1 \approx \ell_2$ ($\mu_1 \approx \mu_2$) while it is positive and increases as η gets larger (see (2.29) and figure 2); it makes the correlation function narrower in $|\ell_1-\ell_2|$.

3.3.2 Quark jet

The MLLA solution of (3.1) reads (see (93) in [1])

$$\frac{\mathcal{C}_q-1}{\mathcal{C}_g-1} \overset{MLLA}{\approx} \frac{N_c}{C_F}\left[1+(b-a)(\phi_{1,\ell}+\phi_{2,\ell})\frac{1+\bar{\Delta}}{2+\bar{\Delta}}\right] \tag{3.14}$$

Inserting (3.5)–(3.8) into (3.14) we get

$$\mathcal{C}_q(\ell_1,\ell_2,Y,\lambda) \overset{MLLA}{\approx} 1+\frac{N_c}{C_F}\Big(\mathcal{C}_g(\ell_1,\ell_2,Y,\lambda)-1\Big)\left[1+(b-a)\gamma_0(e^{\mu_1}+e^{\mu_2})\frac{1+2\cosh(\mu_1-\mu_2)}{2+2\cosh(\mu_1-\mu_2)}\right].$$

which finally reduces (for $Q \gg Q_0 \geq \Lambda_{\rm QCD}$) to

$$\mathcal{C}_q(\ell_1,\ell_2,Y,\lambda) \overset{MLLA}{\approx} 1+\frac{N_c}{C_F}\left[\Big(\mathcal{C}_g(\ell_1,\ell_2,Y,\lambda)-1\Big)+\frac{1}{2}(b-a)\gamma_0\frac{e^{\mu_1}+e^{\mu_2}}{1+\cosh(\mu_1-\mu_2)}\right]. \tag{3.15}$$

3.4 Sensitivity of the quark and gluon jets correlators to the value of λ

Increasing λ translates into taking the limits β, $\Lambda_{\rm QCD} \to 0$ ($Y = \ell + y \ll \lambda$, $Q \gg Q_0 \gg \Lambda_{\rm QCD}$) in the definition of the anomalous dimension via the running coupling constant ($\gamma_0 = \gamma_0(\alpha_s)$, see (44) in [1]). It allows to neglect ℓ, y with respect to λ as follows

$$\gamma_0^2(\ell+y) = \frac{1}{\beta(\ell+y+\lambda)} \overset{\ell+y\ll\lambda}{\approx} \gamma_0^2 = \frac{1}{\beta\lambda}, \tag{3.16}$$

such that γ_0 can be taken as a constant. Estimating (2.4) in the region $\lambda \gg 1 \Leftrightarrow s \ll 1$ needs evaluating the kernel

$$\frac{1}{\nu+s}\left(\frac{\omega\,(\nu+s)}{(\omega+s)\,\nu}\right)^{1/\beta(\omega-\nu)}\left(\frac{\nu}{\nu+s}\right)^{a/\beta}\overset{s\ll 1}{\approx}\frac{1}{\nu}\left(1+\frac{\omega-\nu}{\omega\nu}s\right)^{1/\beta(\omega-\nu)}\left(1-\frac{s}{\nu}\right)^{a/\beta}$$
$$\approx\frac{1}{\nu}\left[1+\frac{1}{\nu}\left(\frac{1}{\omega}-a\right)\frac{s}{\beta}+\frac{1}{2!}\frac{1}{\nu^2}\left(\frac{1}{\omega}-a\right)^2\frac{s^2}{\beta^2}+\frac{1}{3!}\frac{1}{\nu^3}\left(\frac{1}{\omega}-a\right)^3\frac{s^3}{\beta^3}+\cdots\right]. \quad (3.17)$$

Integrating (3.17) over s, using (3.16) and $\int_0^\infty s^n\,e^{-\lambda s}=\frac{n!}{\lambda^n}$, we get

$$\mathcal{G}(\omega,\nu)\approx\frac{1}{\nu}\left[1+\frac{1}{\nu}\left(\frac{1}{\omega}-a\right)\frac{1}{\beta\lambda}+\frac{1}{\nu^2}\left(\frac{1}{\omega}-a\right)^2\left(\frac{1}{\beta\lambda}\right)^2+\frac{1}{\nu^3}\left(\frac{1}{\omega}-a\right)^3\left(\frac{1}{\beta\lambda}\right)^3+\cdots\right]$$
$$=\frac{1}{\nu-\gamma_0^2\,(1/\omega-a)},$$

which, after inverting the Mellin's representation (132) of [1], gives

$$G(\ell,y)\overset{x\ll 1}{\simeq}\exp(2\gamma_0\sqrt{\ell\,y}-a\gamma_0^2 y). \quad (3.18)$$

Taking the same limit in (2.17a) and (2.17b) gives respectively

$$\frac{y-\ell}{y+\ell}\overset{\ell+y\ll\lambda}{\approx}\tanh\mu\Rightarrow\mu=\frac{1}{2}\ln\frac{y}{\ell},\qquad \mu-\upsilon\overset{\ell+y\ll\lambda}{\approx}\frac{1}{2}\frac{y-\ell}{\lambda}\Rightarrow\mu\sim\upsilon. \quad (3.19)$$

Furthermore, we use (3.19) to show how (2.23) reduces to the exponent in (3.18)[3]

$$\phi = \frac{2}{\sqrt{\beta}}\frac{\mu-\upsilon}{\sinh\mu-\sinh\upsilon}\overset{\ell+y\ll\lambda}{\approx}2\gamma_0\sqrt{\ell\,y},$$
$$\left(\frac{\nu_0}{\nu_0+s_0}\right)^{a/\beta} = -\frac{1}{2}\frac{a}{\beta}\ln\left(1+\frac{\ell+y}{\lambda}\right)-\frac{a}{\beta}(\mu-\upsilon)\approx-\frac{1}{2}\frac{a}{\beta}\frac{\ell+y}{\lambda}-\frac{a}{\beta}(\mu-\upsilon)$$
$$\overset{\ell+y\ll\lambda}{\approx}-a\gamma_0^2\,y. \quad (3.20)$$

Thus, since $\mu=\frac{1}{2}\ln\frac{y}{\ell}$ (3.19), (2.30a) and (2.30b) simplify to

$$\psi_\ell\overset{\ell+y\ll\lambda}{\approx}\gamma_0 e^{\mu}=\gamma_0\sqrt{\frac{y}{\ell}},\qquad \psi_y\overset{\ell+y\ll\lambda}{\approx}\gamma_0 e^{-\mu}-a\gamma_0^2=\gamma_0\sqrt{\frac{\ell}{y}}-a\gamma_0^2. \quad (3.21)$$

Therefore, taking the limit $\beta,\,\Lambda_{\rm QCD}\to 0$ ($\lambda\to\infty$) leads to the simplified model described in section 4.2 of [1]. Setting, for the sake of simplicity, $\ell_1\approx\ell_2$ in (3.13)(3.14), where δ_1 vanishes, we obtain, in the high energy limit

$$\mathcal{C}_g(\ell,y)\simeq 1+\frac{1}{3}\left[1-2\left(b-\frac{1}{3}a\right)\psi_\ell(\ell,y)\right],\quad \mathcal{C}_q(\ell,y)\simeq 1+\frac{N_c}{C_F}\left[\frac{1}{3}-\frac{1}{2}\left(\frac{5}{3}a+b\right)\psi_\ell(\ell,y)\right], \quad (3.22)$$

[3] we set $\beta=0$ in (2.30a), (2.30b) and only consider terms $\propto a$

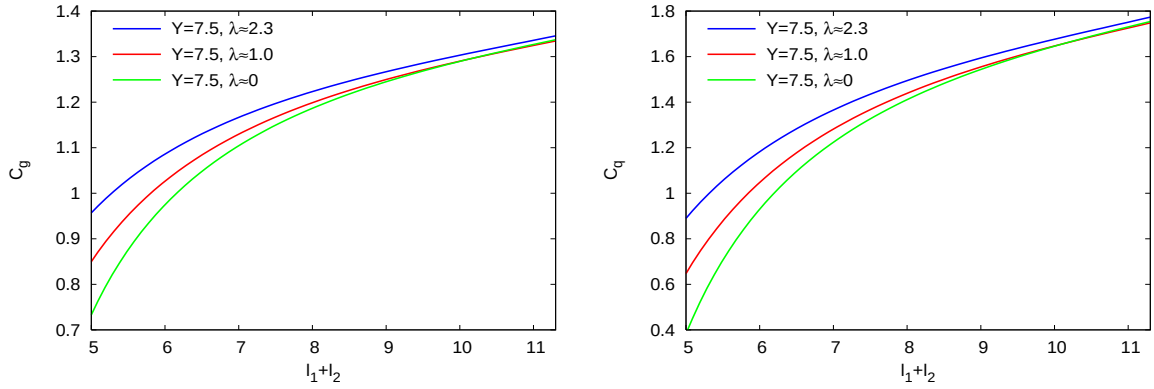

Figure 6: Varying λ at fixed Q_0; $\Lambda_{\rm QCD}$ dependence of $\mathcal{C}_g$ (left) and $\mathcal{C}_q$ (right)

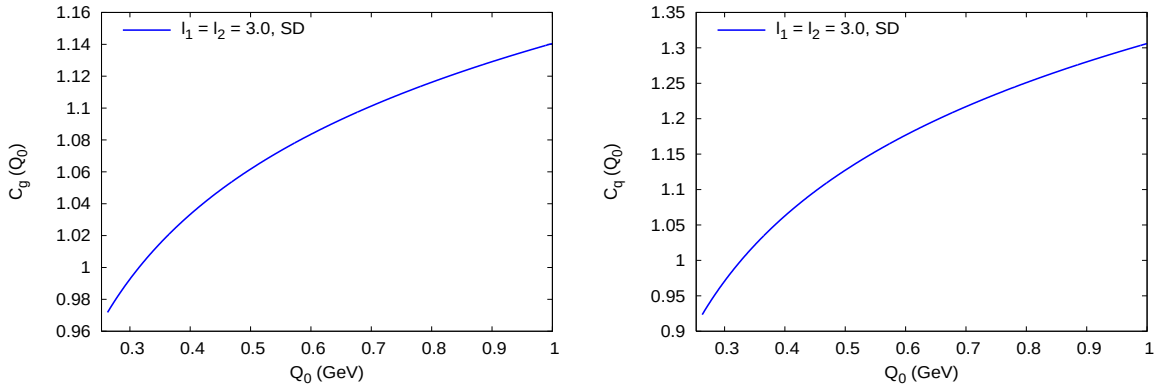

Figure 7: Varying λ at fixed $\Lambda_{\rm QCD} = 253\,MeV$; Q_0-dependence of $\mathcal{C}_g$ (left) and $\mathcal{C}_q$ (right) at $\ell_1 = \ell_2 = 3.0$

where

$$b - \frac{1}{3}a = \frac{1}{18}\left(11 - 8\frac{T_R}{N_c} + 28\frac{T_R}{N_c}\frac{C_F}{N_c} - 24\frac{T_R}{N_c}\frac{C_F^2}{N_c^2}\right) \overset{n_f=3}{\approx} 0.6,$$
$$\frac{5}{3}a + b = \frac{2}{9}\left(11 + \frac{T_R}{N_c} + \frac{T_R}{N_c}\frac{C_F}{N_c} - 6\frac{T_R}{N_c}\frac{C_F^2}{N_c^2}\right) \overset{n_f=3}{\approx} 2.5. \tag{3.23}$$

Thus, when λ increases by decreasing $\Lambda_{\rm QCD}$, $\psi_\ell \propto \gamma_0$ decreases and the correlators (3.22) increase. For LHC, a typical value is $Y = 7.5$ and we compare in figure 6, at fixed Q_0, the limiting case $\lambda \approx 0$ ($Q_0 \approx \Lambda_{\rm QCD} \approx 253\,$MeV) with $\lambda \approx 1.0$ ($\Lambda_{\rm QCD} = 100\,$MeV) and $\lambda \approx 2.3$ ($\Lambda_{\rm QCD} = 25\,$MeV). As predicted by (3.22), the correlation increases when $\Lambda_{\rm QCD} \to 0$ at fixed Q_0.

It is also sensitive to the value of Q_0. As seen in (3.22), since $y = \ln\frac{Q}{Q_0} - \ell$, if one increases Q_0 (since $\Lambda_{\rm QCD}$ is fixed, γ_0 does not change), thereby reducing the available phase space, the correlators increase. This dependence of the correlators at fixed $\Lambda_{\rm QCD}$ is displayed in figure 7 for $0.3\,\text{GeV} \le Q_0 \le 1.0\,\text{GeV}$ at $\ell_1 = \ell_2 = 3.0$ (soft parton).

In the simplified model which leads to (3.22), $\mathcal{C}_g$ and $\mathcal{C}_q$ respectively go to the asymptotic values 4/3 and $1 + N_c/3C_F$. This is however not the case in the general situation $\beta \neq 0$, as can be easily checked by using (2.30a) and (2.30b); for example, near the maximum of the distribution ($\mu \sim v \to 0$), a contribution $\propto \lambda^{3/2}/[(Y+\lambda)^{3/2} - \lambda^{3/2}]$ occurs in the term proportional to β in (3.22) that yields negative values of ψ_ℓ when λ increases.

3.5 Extension of the Fong and Webber expansion; its limit $\lambda = 0$

In the Fong-Webber regime, the energies of the two registered particles stay very close to the peak of the inclusive hump-backed distribution that is, $|\ell_i - \ell_{\max}| \ll \sigma \propto [(Y+\lambda)^{3/2} - \lambda^{3/2}]^{1/2}$ (see (2.22)).

Near the maximum of the single inclusive distribution $\ell_1 \sim \ell_2 \simeq Y/2$ ($\mu, \upsilon \to 0$, see appendix A.2)

$$\lim_{\mu,\upsilon\to 0} C = \left(\frac{\lambda}{Y+\lambda}\right)^{1/2}, \quad \lim_{\mu,\upsilon\to 0} K_i = \frac{3}{2}\frac{v_i^2}{\mu_i^3 - v_i^3}, \quad \lim_{\mu,\upsilon\to 0} \widetilde{Q} = \frac{2}{3} + \frac{1}{3}\left(\frac{\lambda}{Y+\lambda}\right)^{3/2},$$

where C, K_i and $\tilde{Q}$ are defined in (2.31), (A.8) and (2.29). Keeping only the terms linear in μ and the term quadratic in the difference $(\mu_1 - \mu_2)$, one has

$$\bar{\Delta} + \Delta' \overset{\ell_1\sim\ell_2\simeq Y/2}{\simeq} 2 + (\mu_1-\mu_2)^2 - a\gamma_0\,(2+\mu_1+\mu_2) - \beta\gamma_0\left[2 + 3\frac{\lambda^{3/2}}{(Y+\lambda)^{3/2} - \lambda^{3/2}}\right] \quad (3.24)$$

and

$$\delta_1 \overset{\ell_1\sim\ell_2\simeq Y/2}{\simeq} \frac{1}{9}\beta\gamma_0(\mu_1-\mu_2)^2\left[2 + \left(\frac{\lambda}{Y+\lambda}\right)^{3/2}\right]; \quad (3.25)$$

δ_1 can be neglected, since $\gamma_0(\mu_1-\mu_2)^2 \ll (\mu_1-\mu_2)^2 \ll 1$. Then, in the same limit, (3.13), (3.15) become

$$\mathcal{C}_g^0(\ell_1,\ell_2,Y,\lambda) \overset{\ell_1\sim\ell_2\simeq Y/2}{\simeq} 1 + \frac{1 - b\gamma_0(2+\mu_1+\mu_2)}{3 + (\mu_1-\mu_2)^2 - a\gamma_0(2+\mu_1+\mu_2) - \beta\gamma_0\left[2 + 3\dfrac{\lambda^{3/2}}{(Y+\lambda)^{3/2} - \lambda^{3/2}}\right]}, \quad (3.26)$$

$$\mathcal{C}_q^0(\ell_1,\ell_2,Y,\lambda) \overset{\ell_1\sim\ell_2\simeq Y/2}{\simeq} 1 + \frac{N_c}{C_F}\left[\left(\mathcal{C}_g^0(\ell_1,\ell_2,Y,\lambda) - 1\right) + \frac{1}{4}(b-a)\gamma_0\,(2+\mu_1+\mu_2)\right]. \quad (3.27)$$

Using (A.4) one has

$$(\mu_1-\mu_2)^2 \simeq 9\frac{Y+\lambda}{\left[(Y+\lambda)^{3/2} - \lambda^{3/2}\right]^2}(\ell_1-\ell_2)^2, \quad \mu_1+\mu_2 \simeq 3\frac{(Y+\lambda)^{1/2}}{(Y+\lambda)^{3/2} - \lambda^{3/2}}\,[Y - (\ell_1+\ell_2)]$$

such that the expansion of (3.26), (3.27) in $\gamma_0 \propto \sqrt{\alpha_s}$ reads

$$\begin{aligned}\mathcal{C}_g^0(\ell_1,\ell_2,Y,\lambda) \simeq\ & \frac{4}{3} - \left(\frac{(Y+\lambda)^{1/2}(\ell_1-\ell_2)}{(Y+\lambda)^{3/2} - \lambda^{3/2}}\right)^2 \\ & + \left(\frac{2}{3} + \frac{(Y+\lambda)^{1/2}\,Y}{(Y+\lambda)^{3/2} - \lambda^{3/2}}\right)\left(\frac{1}{3}a - b\right)\gamma_0 + \frac{1}{3}\left(\frac{2}{3} + \frac{\lambda^{3/2}}{(Y+\lambda)^{3/2} - \lambda^{3/2}}\right)\beta\gamma_0 \\ & + \left(b - \frac{1}{3}a\right)\left(\frac{(Y+\lambda)^{1/2}\,(\ell_1+\ell_2)}{(Y+\lambda)^{3/2} - \lambda^{3/2}}\right)\gamma_0 + \mathcal{O}(\gamma_0^2), \end{aligned} \quad (3.28)$$

$$\mathcal{C}_q^0(\ell_1,\ell_2,Y,\lambda) \simeq 1+\frac{N_c}{3C_F}+\frac{N_c}{C_F}\Bigg[-\left(\frac{(Y+\lambda)^{1/2}(\ell_1-\ell_2)}{(Y+\lambda)^{3/2}-\lambda^{3/2}}\right)^2$$
$$-\frac{1}{4}\left(\frac{2}{3}+\frac{(Y+\lambda)^{1/2}\,Y}{(Y+\lambda)^{3/2}-\lambda^{3/2}}\right)\left(\frac{5}{3}a+b\right)\gamma_0+\frac{1}{3}\left(\frac{2}{3}+\frac{\lambda^{3/2}}{(Y+\lambda)^{3/2}-\lambda^{3/2}}\right)\beta\gamma_0$$
$$+\frac{1}{4}\left(\frac{5}{3}a+b\right)\left(\frac{(Y+\lambda)^{1/2}\,(\ell_1+\ell_2)}{(Y+\lambda)^{3/2}-\lambda^{3/2}}\right)\gamma_0\Bigg]+\mathcal{O}(\gamma_0^2). \tag{3.29}$$

Therefore, near the hump of the single inclusive distribution, (3.13), (3.15) behave as a linear functions of the sum $(\ell_1+\ell_2)$ and as a quadratic functions of the difference $(\ell_1-\ell_2)$. At the limit $\lambda=0$, one recovers the Fong-Webber expression [3].

3.6 Comparison with the exact solution of the evolution equations: $\lambda = 0$

In figures 8 we compare the SD evaluation of the gluon correlator with the exact solution of [1] at $\lambda=0$. The difference comes from sub-leading corrections of order γ_0^2 that are not present in (3.13). For example, $-\beta\gamma_0^2\approx -0.2$ at $Y=5.2$ occurring in the exact solution (69) of [1] is not negligible but is absent in (3.13) and (3.15). That is why, the SD MLLA curve lies slightly above the one of [1] at small $\ell_1+\ell_2$. The mismatch becomes smaller at $Y=7.5$, since $-\beta\gamma_0^2\approx -0.13$. However, when $\ell_1+\ell_2$ increases, the solution of [1] takes over, which can be explained by comparing the behavior of the SD MLLA δ_1 obtained in (3.12) and δ_c, $\tilde{\delta}_c$ in [1]. Namely, while δ_1 remains positive and negligible for $\ell_1\approx\ell_2$, δ_c, $\tilde{\delta}_c$ decrease and get negative when $\ell_1+\ell_2\to 2Y$, see figure 9 (left), which makes the correlations slightly bigger in this region. As $|\ell_1-\ell_2|$ increases, δ_1 is seen in figure 9 (right) to play the same role as $\delta_c,\tilde{\delta}_c$ do in the solution [1] and therefore, to decrease the correlation. The agreement between both methods improves as the energy scale increases. A similar behavior holds for the quark correlator.

In [1], strong cancellations between the MLLA δ_1 and the NMLLA δ_2 were seen to take place, giving very small δ_c and $\tilde{\delta}_c$; this eased the convergence of the iterative method but raised questions concerning the relative size of MLLA and NMLLA corrections and the validity of the perturbative expansion. However, since δ_1 is itself, there, entangled with *some* NMLLA corrections, no definitive conclusions could be drawn. The present work and figure 9, by showing that, below, δ_c and $\tilde{\delta}_c$ of [1] play the same role as the *pure MLLA* δ_1 which is now calculated, suggests (though it is not a demonstration) that the perturbative series is safe. It is indeed compatible with the following scheme: in [1], the pure MLLA part of δ_1 is the same as that in the present work; the cancellations in [1] occur between NMLLA corrections included in δ_1 and δ_2; these are eventually of the same order of magnitude as MLLA terms, but they are only parts of all NMLLA corrections; this leaves the possibility that the sum of all NMLLA corrections to δ_1 and all NMLLA terms of δ_2 are separately smaller than the pure MLLA terms of δ_1, that is that strong cancellations occur *between NMLLA corrections*, the ones included, because of the logic of the calculation, in [1], and those which were not be taken into account.

JHEP09(2006)014

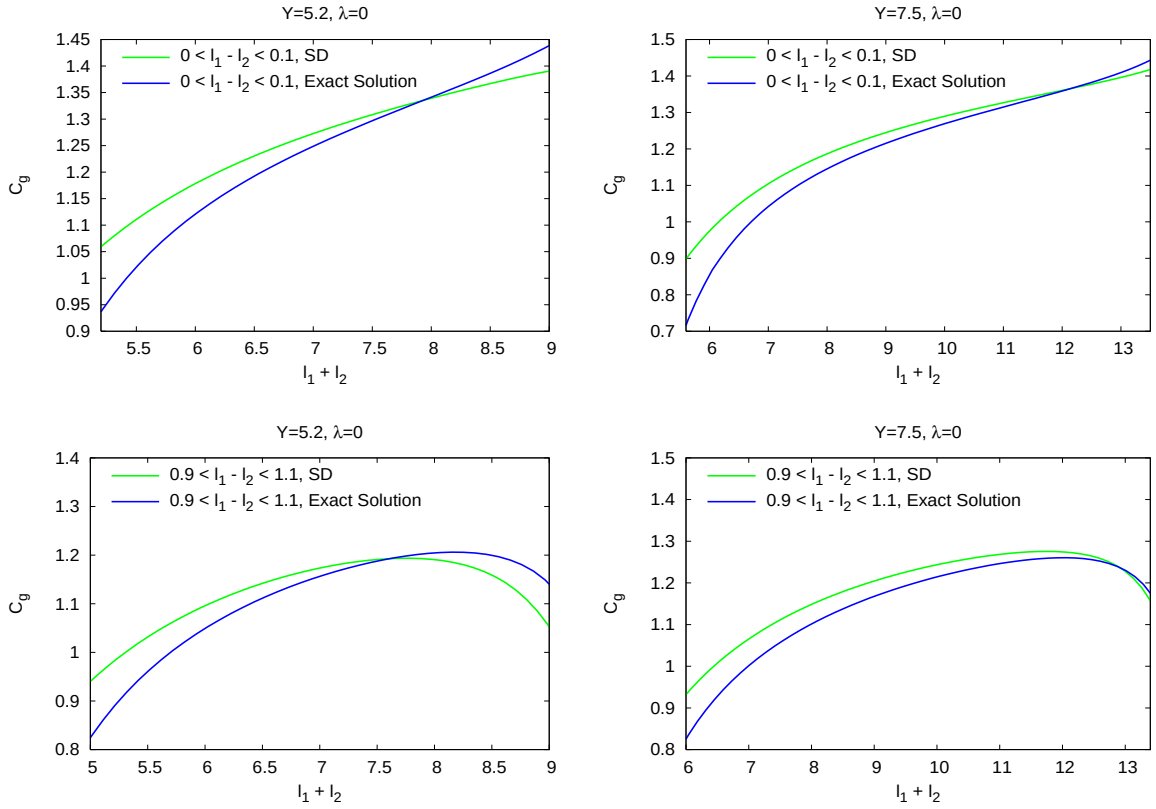

Figure 8: Comparison between correlators given by SD and in [1], at $\lambda = 0$.

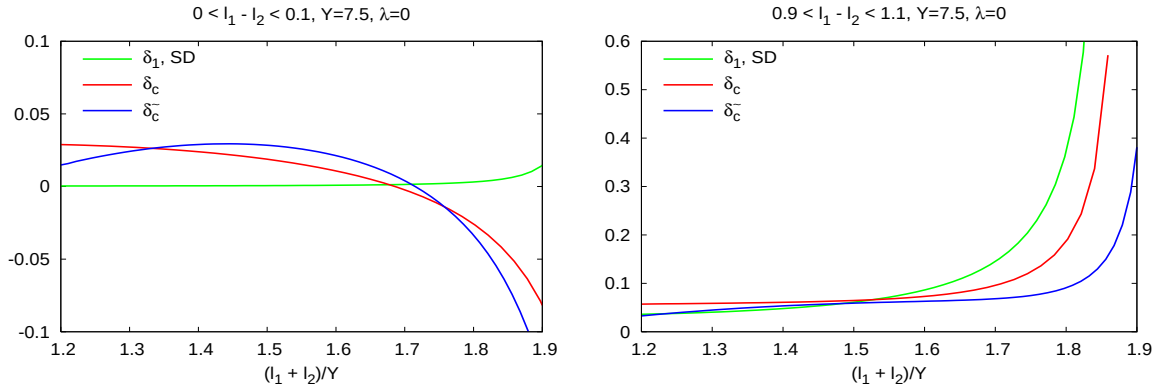

Figure 9: Comparison between the SD δ_1 and δ_c, $\tilde{\delta}_c$ of [1] at $Y = 7.5$, $\lambda = 0$.

3.7 Comparison with Fong-Webber and LEP-I data; how $\lambda = 0$ is favored

Let us consider, at the Z^0 peak $Y = 5.2$ ($E\Theta = 91.2\,\mathrm{GeV}$ at LEP-I energy), the process $e^+e^- \to q\bar{q}$. As can be induced from figure 8, the results obtained in the present work by the (approximate) SD method are very close to the ones obtained in subsection 6.5 of [1] by the exact solution of the evolution equations. Accordingly, the same comparison as in [1] holds with respect to both Fong & Webber's results [3] and OPAL data [6].

JHEP09(2006)014

It is also noticeable that, since, at $\lambda = 0$, correlations already lye above (present) experimental curves, and since an increase of λ tends to increase the predictions, the limiting spectrum stays the best candidate to bring agreement with experiments.

4. Conclusion

Let us, in a few words, summarize the achievements, but also the limitations of the two methods that have been used respectively in [1] (exact solution of MLLA evolution equations) and in the present work (steepest descent approximate evaluation of their solutions).

Achievements are threefold:

- in [1], MLLA evolution equations for 2-particle correlations have been deduced at small x and at any λ; their (iterative) solution can unfortunately only be expressed analytically at the limit $\lambda \to 0$;
- by the steepest descent method, which is an approximate method, analytical expressions for the spectrum could instead be obtained for $\lambda \neq 0$, which enabled to calculate the correlation at the same level of generality;
- one could move away from the peak of the inclusive distribution.

So doing, the limitations of the work of Fong & Webber have vanished. Their results have been recovered at the appropriate limits.

The two methods numerically agree remarkably well, despite an unavoidable entanglement of MLLA + some NMLLA corrections in the first one.

The limitations are the following:

- the uncontrollable increase of α_s when one goes to smaller and smaller transverse momenta: improvements in this directions mainly concern the inclusion of non-perturbative contributions;
- departure from the limiting spectrum: it cannot of course appear as a limitation, but we have seen that increasing the value of λ, by increasing the correlations, does not bring better agreement with present data; it confirms thus, at present, that the limiting spectrum is the best possibility;
- the LPHD hypothesis: it works surprisingly well for inclusive distributions; only forthcoming data will assert whether its validity decreases when one studies less inclusive processes (like correlations);
- last, the limitation to small x: it is still quite drastic; departing from this limit most probably lye in the art of numerical calculations, which makes part of forthcoming projects.

Expectations rest on experimental data, which are being collected at the Tevatron, and which will be at LHC. The higher the energy, the safer perturbative QCD is, and the better the agreement should be with our predictions. The remaining disagreement (but

JHEP09(2006)014

much smaller than Fong-Webber's) between predictions and LEP-1 results for 2-particle correlations stands as an open question concerning the validity of the LPHD hypothesis for these observables which are not "so" inclusive as the distributions studied in [5]. The eventual necessity to include NMLLA corrections can only be decided when new data appear.

Acknowledgments

It is a pleasure to thank Yuri Dokshitzer for enticing me towards the steepest descent method and for showing me its efficiency with simple examples. I am grateful to Bruno Machet for his help and advice and to Gavin Salam for helping me in numerically inverting formula (2.17a).

A. Double derivatives and determinant

A.1 Demonstration of eq. (2.19)

We conveniently rewrite (2.11a) and (2.11b) in the form

$$\frac{\partial\phi}{\partial\omega} = \frac{2\omega-\nu}{\omega-\nu}\ell + \frac{\nu}{\omega-\nu} - \frac{\phi}{\omega-\nu} - \lambda\frac{\nu+2s_0}{\omega-\nu} + \frac{1}{\beta\omega(\omega-\nu)}, \tag{A.1}$$

$$\frac{\partial\phi}{\partial\nu} = \frac{\omega-2\nu}{\omega-\nu}y - \frac{\omega}{\omega-\nu} + \frac{\phi}{\omega-\nu} + \lambda\frac{\omega+2s_0}{\omega-\nu} - \frac{1}{\beta\nu(\omega-\nu)}. \tag{A.2}$$

The Taylor expansion of (2.10) in (2.9) reads

$$\begin{aligned}\phi(\omega,\nu,\ell,y) \approx\ & \phi(\omega_0,\nu_0,\ell,y) + \frac{1}{2}\frac{\partial^2\phi}{\partial\omega^2}(\omega_0,\nu_0)(\omega-\omega_0)^2 \\ & + \frac{1}{2}\frac{\partial^2\phi}{\partial\nu^2}(\omega_0,\nu_0)(\nu-\nu_0)^2 + \frac{\partial^2\phi}{\partial\omega\partial\nu}(\omega_0,\nu_0)\,(\omega-\omega_0)(\nu-\nu_0).\end{aligned} \tag{A.3}$$

The expressions of the second derivatives follow directly from (A.1) and (A.2)

$$\begin{aligned}\frac{\partial^2\phi}{\partial\omega^2} &= -\frac{\nu}{(\omega-\nu)^2}(\ell{+}y{+}\lambda) + \frac{\phi}{(\omega-\nu)^2} - \frac{2\omega-\nu}{\beta\omega^2(\omega-\nu)^2} + \frac{4}{\beta(\omega-\nu)^2(2s_0+\omega+\nu)},\\ \frac{\partial^2\phi}{\partial\nu^2} &= -\frac{\omega}{(\omega-\nu)^2}(\ell{+}y{+}\lambda) + \frac{\phi}{(\omega-\nu)^2} + \frac{\omega-2\nu}{\beta\nu^2(\omega-\nu)^2} + \frac{4}{\beta(\omega-\nu)^2(2s_0+\omega+\nu)},\\ \frac{\partial^2\phi}{\partial\omega\partial\nu} &= \frac{\omega}{(\omega-\nu)^2}(\ell{+}y{+}\lambda) - \frac{\phi}{(\omega-\nu)^2} + \frac{1}{\beta\omega(\omega-\nu)^2} - \frac{4}{\beta(\omega-\nu)^2(2s_0+\omega+\nu)}.\end{aligned}$$

Eq. (2.9) and its solution can be written in the form

$$G \simeq \iint d^2v\, e^{-\frac{1}{2}v^T A v} = \frac{2\pi}{\sqrt{\mathrm{Det}\ A}}$$

where

$$v=(\omega,\nu), \quad v^T = \begin{pmatrix}\omega\\ \nu\end{pmatrix}, \quad \mathrm{Det}\,A = \mathrm{Det}\begin{pmatrix}\frac{\partial^2\phi}{\partial\omega^2} & \frac{\partial^2\phi}{\partial\omega\partial\nu}\\ \frac{\partial^2\phi}{\partial\nu\partial\omega} & \frac{\partial^2\phi}{\partial\nu^2}\end{pmatrix} = \frac{\partial^2\phi}{\partial\omega^2}\frac{\partial^2\phi}{\partial\nu^2} - \left(\frac{\partial^2\phi}{\partial\omega\partial\nu}\right)^2.$$

An explicit calculation gives

$$\mathrm{Det}\, A = (\ell + y + \lambda)^2 \left[\frac{\beta(\omega+\nu)\phi - 4}{(\omega-\nu)^2} + \frac{4(\omega+\nu)}{(\omega-\nu)^2(2s_0+\omega+\nu)} \right]$$

which, by using (2.15) leads to (2.19).

A.2 Det A (see eq. (2.19)) around the maximum

This is an addendum to subsection 2.3. $\ell_{\max}$ written in (2.21) is close to the DLA value $Y/2$ [7–9]. We then have $\mu \sim \upsilon \to 0$ for $\ell \approx y \simeq Y/2$. In this limit, (2.17a) and (2.17b) respectively translate into

$$Y - 2\ell \overset{\mu,\upsilon\to 0}{\approx} \frac{2}{3} \frac{(Y+\lambda)^{3/2} - \lambda^{3/2}}{(Y+\lambda)^{1/2}}\, \mu, \quad \upsilon \overset{\mu,\upsilon\to 0}{\approx} \sqrt{\frac{\lambda}{Y+\lambda}}\mu, \tag{A.4}$$

while

$$\frac{\partial \mu}{\partial \ell} \simeq -3 \frac{(Y+\lambda)^{1/2}}{(Y+\lambda)^{3/2} - \lambda^{3/2}} \tag{A.5}$$

should be used to get (2.22). An explicit calculation gives

$$\lim_{\mu,\upsilon\to 0} \sqrt{\frac{\beta^{1/2}(Y+\lambda)^{3/2}}{\pi\, \mathrm{Det}\, A(\mu,\upsilon)}} = \left(\frac{3}{\pi\sqrt{\beta}\left[(Y+\lambda)^{3/2} - \lambda^{3/2}\right]} \right)^{1/2},$$

where

$$\mathrm{Det}\, A \overset{\mu,\upsilon\to 0}{\approx} \beta(Y+\lambda)^3 \frac{(\mu-\upsilon)\left(1+\frac{1}{2}\mu^2\right)\left(1+\frac{1}{2}\upsilon^2\right) + \left(1+\frac{1}{2}\mu^2\right)\left(\upsilon+\frac{1}{6}\upsilon^3\right) - \left(\mu+\frac{1}{6}\mu^3\right)\left(1+\frac{1}{2}\upsilon^2\right)}{\mu^3}$$

$$\simeq \frac{1}{3}\beta(Y+\lambda)^3 \left(1 - \frac{\upsilon^3}{\mu^3}\right) = \frac{1}{3}\beta(Y+\lambda)^3 \left[1 - \left(\frac{\lambda}{Y+\lambda}\right)^{3/2}\right]. \tag{A.6}$$

A.3 The functions $L(\mu,\upsilon)$, $K(\mu,\upsilon)$ in eq. (2.26)

An explicit calculation gives

$$L(\mu,\upsilon) = \frac{3}{2}\frac{\cosh\mu}{\sinh\mu} - \frac{1}{2}\frac{(\mu-\upsilon)\cosh\upsilon\sinh\mu + \sinh\upsilon\sinh\mu}{(\mu-\upsilon)\cosh\mu\cosh\upsilon + \cosh\mu\sinh\upsilon - \sinh\mu\cosh\upsilon}, \tag{A.7}$$

and

$$K(\mu,\upsilon) = -\frac{1}{2}\sinh\upsilon \frac{(\mu-\upsilon)\cosh\mu - \sinh\mu}{(\mu-\upsilon)\cosh\mu\cosh\upsilon + \cosh\mu\sinh\upsilon - \sinh\mu\cosh\upsilon}. \tag{A.8}$$

A.4 A consistency check

Let us verify that the evolution equation (2.2) is satisfied by (2.20) within the MLLA accuracy. Differentiating (2.2) with respect to ℓ, y yields the equivalent differential equation

$$G_{\ell y} = \gamma_0^2 \left(G - aG_\ell\right) + \mathcal{O}\left(\gamma_0^4 G\right)$$

that can be rewritten in the form

$$\psi_\ell\psi_y + \psi_{\ell y} \;=\; \gamma_0^2\,(1 - a\psi_\ell) \;+\; \mathcal{O}\big(\gamma_0^4\big); \tag{A.9}$$

we have neglected next-to-MLLA corrections $\mathcal{O}(\gamma_0^4)$ (of relative order γ_0^2) coming from differentiating the coupling γ_0^2 in the sub-leading ("hard correction") term $\propto a$.

We have to make sure that (A.9) holds including the terms $\mathcal{O}(\gamma_0^3)$. In the sub-leading terms we can set $\psi \to \varphi$ (see (2.25)):

$$(\varphi_\ell + \delta\psi_\ell)(\varphi_y + \delta\psi_y) + \varphi_{\ell y} = \gamma_0^2(1 - a\varphi_\ell). \tag{A.10}$$

Isolating correction terms and casting them all on the l.h.s. of the equation we get

$$a\gamma_0^2\varphi_\ell + [\,\varphi_\ell\delta\psi_y + \varphi_y\delta\psi_\ell\,] + \varphi_{\ell y} \;=\; \gamma_0^2 - \varphi_\ell\varphi_y. \tag{A.11}$$

By the definition (2.25) of the saddle point we conclude that the r.h.s. of (A.11) is zero such that we have

$$\omega_0 a\gamma_0^2 + [\,\omega_0\delta\psi_y + \nu_0\delta\psi_\ell\,] + \frac{d\omega_0}{dy} \;=\; 0\,, \tag{A.12}$$

that is,

$$\omega_0\left(a\gamma_0^2 + \delta\psi_y\right) + \nu_0\delta\psi_\ell + \frac{d\omega_0}{dy} \;=\; 0\,. \tag{A.13}$$

First, we select the terms $\propto a$:

$$\begin{aligned}
&a\gamma_0^3\left[-\frac{1}{2}\widetilde{Q} - \frac{1}{2}\tanh\upsilon\, e^{\mu} + \frac{1}{2}\tanh\upsilon\coth\mu\, e^{\mu} + \frac{1}{2}\tanh\upsilon\coth\mu\,\widetilde{Q}\right.\\
&\left.+\frac{1}{2}\widetilde{Q} - \frac{1}{2}\tanh\upsilon\, e^{-\mu} - \frac{1}{2}\tanh\upsilon\coth\mu\, e^{-\mu} - \frac{1}{2}\tanh\upsilon\coth\mu\,\widetilde{Q}\right]\\
&= a\gamma_0^3\,[-\tanh\upsilon\cosh\mu + \tanh\upsilon\coth\mu\sinh\mu] \equiv 0.
\end{aligned}$$

From (2.15) one deduces

$$\frac{d\omega_0}{dy} = \frac{1}{2}\beta\gamma_0^3\widetilde{Q},$$

that is inserted in (A.13) such that, for terms $\propto \beta$, we have

$$\begin{aligned}
&-\beta\gamma_0^3\left[\frac{1}{2}e^{\mu} + \frac{1}{2}\tanh\upsilon\Big(1{+}K\Big)e^{\mu} - \frac{1}{2}C\, e^{\mu} - \frac{1}{2}C\widetilde{Q} + \frac{1}{2}e^{-\mu} + \frac{1}{2}\tanh\upsilon\Big(1{+}K\Big)e^{-\mu}\right.\\
&\left.+\frac{1}{2}C\, e^{-\mu} + \frac{1}{2}C\widetilde{Q}\right] = -\beta\gamma_0^3\left[\cosh\mu + \tanh\upsilon\cosh\mu\Big(1{+}K\Big) - C\sinh\mu - \frac{1}{2}\widetilde{Q}\right],
\end{aligned}$$

which gives

$$-\beta\gamma_0^3\left[\cosh\mu - \sinh\mu\, L - \frac{1}{2}\widetilde{Q}\right].$$

Constructing (see (2.29) and appendix A.3)

$$\begin{aligned}
\widetilde{Q}(\mu,\upsilon) - 2\cosh\mu \;&=\; -3\cosh\mu + \sinh\mu\,\frac{(\mu-\upsilon)\cosh\upsilon\sinh\mu + \sinh\upsilon\sinh\mu}{(\mu-\upsilon)\cosh\mu\cosh\upsilon + \cosh\mu\sinh\upsilon - \sinh\mu\cosh\upsilon}\\
&=\; -2\sinh\mu L(\mu,\upsilon)
\end{aligned}$$

we have

$$-\beta\gamma_0^3\left[\cosh\mu - \sinh\mu\, L - \frac{1}{2}\widetilde{Q}\right] \equiv 0.$$

B. Analytical expression of $\Delta'(\mu_1,\mu_2)$ obtained from eq. (3.10)

Replacing (2.30a)(2.30b) in (3.10) and neglecting terms of relative order $\mathcal{O}(\gamma_0^3)$ which are beyond the MLLA accuracy, we obtain

$$\begin{aligned}
\Delta' &= \frac{e^{-\mu_1}\delta\psi_{2,\ell} + e^{-\mu_2}\delta\psi_{1,\ell} + e^{\mu_1}\delta\psi_{2,y} + e^{\mu_2}\delta\psi_{1,y}}{\gamma_0} \\
&= -a\gamma_0\Big[e^{\mu_1} + e^{\mu_2} - \sinh(\mu_1-\mu_2)(\widetilde{Q}_1 - \widetilde{Q}_2) + \cosh\mu_1\tanh\upsilon_2 + \cosh\mu_2\tanh\upsilon_1 \\
&\quad - \sinh\mu_1\tanh\upsilon_2\coth\mu_2 - \sinh\mu_2\tanh\upsilon_1\coth\mu_1 \\
&\quad + \sinh(\mu_1-\mu_2)\Big(\tanh\upsilon_1\coth\mu_1\widetilde{Q}_1 - \tanh\upsilon_2\coth\mu_2\widetilde{Q}_2\Big)\Big] \\
&\quad -\beta\gamma_0\Big[\Big(\cosh\mu_1 - \sinh\mu_1 C_2\Big) + \Big(\cosh\mu_2 - \sinh\mu_2 C_1\Big) + \sinh(\mu_1-\mu_2)(C_1\widetilde{Q}_1 - C_2\widetilde{Q}_2) \\
&\quad + \cosh\mu_1\tanh\upsilon_2\Big(1+K_2\Big) + \cosh\mu_2\tanh\upsilon_1\Big(1+K_1\Big)\Big]\,. \qquad \text{(B.1)}
\end{aligned}$$

References

[1] R. Perez-Ramos, *Two-particle correlations inside one jet at "modified leading logarithmic approximation" of quantum chromodynamics, I. Exact solution of the evolution equations at small x*, *JHEP* **06** (2006) 019 [hep-ph/0605083] and references therein.

[2] Y.L. Dokshitzer, V.A. Khoze and S.I. Troyan, *Inclusive particle spectra from QCD cascades*, *Int. J. Mod. Phys.* **A 7** (1992) 1875.

[3] C.P. Fong and B.R. Webber, *Two particle correlations at small x in QCD jets*, *Phys. Lett.* **B 241** (1990) 255; *One and two particle distributions at small x in QCD jets*, *Nucl. Phys.* **B 355** (1991) 54.

[4] Y.L. Dokshitzer, V.A. Khoze, S.I. Troyan and A.H. Mueller, *QCD coherence in high-energy reactions*, *Rev. Mod. Phys.* **60** (1988) 373.

[5] R. Perez-Ramos and B. Machet, *MLLA inclusive hadronic distributions inside one jet at high energy colliders*, *JHEP* **04** (2006) 043 [hep-ph/0512236].

[6] OPAL collaboration, P.D. Acton et al., *A study of two particle momentum correlations in hadronic Z0 decays*, *Phys. Lett.* **B 287** (1992) 401.

[7] Y.L. Dokshitzer, V.S. Fadin and V.A. Khoze, *On the sensitivity of the inclusive distributions in parton jets to the coherence effects in QCD gluon cascades*, *Z. Physik* **C 18** (1983) 37.

[8] Y.L. Dokshitzer, V.A. Khoze, A.H. Mueller and S.I. Troyan, *Basics of Perturbative QCD*, Editions Frontières, Paris 1991.

[9] V.A. Khoze and W. Ochs, *Perturbative QCD approach to multiparticle production*, *Int. J. Mod. Phys.* **A 12** (1997) 2949 [hep-ph/9701421].

[10] C.P. Fong and B.R. Webber, *Higher order QCD corrections to hadron energy distributions in jets*, *Phys. Lett.* **B 229** (1989) 289.

JHEP09(2006)014